Check for updates

Hindawi
Adsorption Science & Technology
Volume 2022, Article ID 4482263, 14 pages
https://doi.org/10.1155/2022/4482263

Research Article

Physicochemical Modeling of the Adsorption of Pharmaceuticals on MIL-100-Fe and MIL-101-Fe MOFs

Fátima Gisela Quintero-Álvarez,[1] **Cintia Karina Rojas-Mayorga**,[2] **Didilia Ileana Mendoza-Castillo**,[1,3] **Ismael Alejandro Aguayo-Villarreal**,[2] **and Adrián Bonilla-Petriciolet**[1]

[1]*Instituto Tecnológico de Aguascalientes, 20256 Aguascalientes, Mexico*
[2]*Universidad de Colima, 28400 Colima, Mexico*
[3]*CONACYT, 03940 Ciudad de México, Mexico*

Correspondence should be addressed to Adrián Bonilla-Petriciolet; petriciolet@hotmail.com

Received 21 December 2021; Revised 15 January 2022; Accepted 17 February 2022; Published 8 March 2022

Academic Editor: Hesham Hamad

Copyright © 2022 Fátima Gisela Quintero-Álvarez et al. This is an open access article distributed under the Creative Commons Attribution License, which permits unrestricted use, distribution, and reproduction in any medium, provided the original work is properly cited.

The adsorption of naproxen (NAP), diclofenac (DFC), and acetaminophen (APAP) molecules from aqueous solutions using MIL-100-Fe and MIL-101-Fe metal organic frameworks (MOFs) has been analyzed and modeled. Adsorption isotherms of these pharmaceuticals were experimentally quantified at 30 and 40°C and pH 7. Textural parameters and surface chemistry of these MOFs were analyzed, and results were utilized to explain the pharmaceutical adsorption mechanism. Density Functional Theory (DFT) calculations were performed to understand the reactivity of pharmaceutical molecules, and a statistical physics model was employed to calculate the main physicochemical parameters related to the adsorption mechanism. Results showed that the adsorption of these pharmaceuticals on MOFs was multimolecular and exothermic. Both MOFs displayed the highest adsorption capacities, up to 2.19 and 1.71 mmol/g, for NAP and DFC molecules, respectively. MIL-101-Fe showed better pharmaceutical adsorption properties than MIL-100-Fe due to its highest content of Fe-O clusters and mesopore volume. Adsorption mechanism of these organic molecules could involve hydrogen bond, van der Waals forces, and electrostatic interactions with MOF surfaces. In particular, MIL-101-Fe MOF is a promising material to prepare composites with competitive adsorption capacities for facing the water pollution caused by pharmaceutical compounds.

1. Introduction

In recent years, the literature has documented an increment of the water pollution caused by emerging compounds [1]. They are unregulated pollutants by the environmental legislation that include an extensive variety of chemicals such as pharmaceuticals, personal hygiene products, and surfactants [1]. In particular, the release of pharmaceutical molecules in the environment is a relevant issue since they can affect significantly the human health causing, for example, carcinogenesis, teratogenesis, and mutagenicity even at very low concentrations (i.e., from μg/L to ng/L) [2–5]. Diclofenac (DFC), naproxen (NAP), and acetaminophen (APAP) are nonsteroidal anti-inflammatory drugs that stand out due to their worldwide prescription for human healthcare [6, 7]. NAP is employed for the treatment of osteoarthritis, rheumatoid arthritis, and migraine and to reduce inflammation and fever [7, 8]. DFC is a widely used pharmaceutical to minimize pain and inflammation caused by ankylosing spondylitis, rheumatoid arthritis, and osteoporosis [9]. This drug is commonly identified as a water pollutant in environmental samples [7]. APAP is also an anti-inflammatory, antipyretic, and analgesic drug [10]. Overall, these pharmaceutical molecules can reach wastewater via the human excreta and by their inappropriate disposal after the drug expiration. Different studies have concluded that these

organic molecules can persist in the environment for a long time due to their resistance to biodegradability and stability to heat and light [11, 12].

The control and reduction of concentrations of pharmaceutical pollutants in the environment, and especially in water resources, can be performed via adsorption [13, 14] or using other treatment methods like photodegradation [15, 16]. Particularly, the removal of pharmaceutical molecules via adsorption processes can offer additional economical and technical advantages, and consequently, it is necessary to study the application of novel adsorbents to consolidate its application at industrial level. In this direction, the metal organic frameworks (MOFs) are interesting adsorbents with promising potential for wastewater treatment including the pharmaceutical depollution due to their surface area, controllable pore size (in micro and mesoporous domains), structural versatility, and composition [17–19]. There is a wide spectrum of metals and organic ligands that can be used for the preparation of MOFs, thus offering the possibility to obtain materials with different physicochemical characteristics and adsorption properties. Research on MOFs has indicated that their adsorption capacity to remove organic molecules is determined by their textural parameters (surface area and pore size) and surface functionalities. These physicochemical properties influence the π-π interactions between the aromatic parts of the linker on the MOF structure and the organic molecules besides the electrostatic adsorbent–adsorbate interactions [20, 21]. Particularly, MIL-100-Fe MOF has been suggested as a promising material for liquid-phase adsorption due to its hydrothermal stability, surface area, and pore volume [22]. It has been utilized successfully as an adsorbent of organic pollutants and heavy metals from liquid phase [23, 24]. In this direction, MIL-101-Fe is another interesting MOF that has been proved as an adsorbent of various toxic chemicals due to the affinity of saturated or unsaturated metal sites [24]. Several studies on the water pollutant adsorption via MOFs have focused mainly on the assessment and improvement of the adsorption capacities of these materials including the preparation of composites. However, the discussion of the adsorbent-adsorbate interactions and physicochemical parameters related to the adsorption mechanism is usually excluded in these studies. Note that the structure of adsorbate molecules (e.g., molecular size, functional groups, polarity, and solubility) could also have a significant impact on the MOF adsorption performance [25, 26]. Therefore, the analysis and interpretation of the adsorption mechanism of pharmaceuticals on MOFs and the impact of their molecular properties are necessary to improve the application of these materials and to tailor their properties with the aim of enhancing the adsorption capacities in water depollution.

Under this perspective, this study reports the modeling and analysis of the physicochemical parameters of the adsorption of pharmaceutical molecules on MIL-100-Fe and MIL-101-Fe MOFs. These materials were synthesized and employed to adsorb DFC, NAP, and APAP as target pharmaceutical molecules from aqueous solutions. These MOFs were characterized and their adsorption properties were determined experimentally at 30–40°C and pH 7. The physicochemical parameters associated to the adsorption mechanism of these pharmaceuticals were calculated via the statistical physics-based modeling. Therefore, this study contributes with new experimental data and theoretical insights on the application of MOFs for the adsorption of pharmaceuticals molecules from aqueous solutions.

2. Methodology

2.1. Synthesis and Characterization of MOFs. MIL-100-Fe and MIL-101-Fe MOFs were prepared and employed to analyze the adsorption of different pharmaceutical molecules from aqueous solutions. MIL-100-Fe was synthetized with 1.76 g of $Fe(NO_3)_3{\cdot}9H_2O$ and 0.57 g of H_3BTC (trimesic acid). The organic linker and metal source were dissolved in 20 mL of deionized water and stirred well for 1 h. The final solution was submitted to a thermal treatment at 160°C for 12 h using a Teflon-lined stainless-steel autoclave. The solid product obtained from the reaction was separated via centrifugation, washed several times with deionized water and ethanol, and finally dried at 80°C for 24 h. The preparation of MIL-101-Fe was performed with 0.675 g of $FeCl_3{\cdot}6H_2O$ and 0.206 g of H_2BDC (terephthalic acid), which were dissolved in 30 mL of DMF. The thermochemical conversion of this solution was done at 110°C for 20 h with the Teflon-lined stainless-steel autoclave. The final solid product was also separated via centrifugation, washed with ethanol, and dried at 80°C and 24 h. Nanosized MOF particles were used in all the pharmaceutical adsorption studies reported in this paper.

Samples of these MOFs were characterized to determine their main surface and textural properties. Surface functional groups were identified by Fourier-transform infrared (FTIR) spectroscopy with a Thermo Nicolet Is10 FTIR spectrometer (Thermo Scientific). Spectra were recorded with KBr-based sample pellets in the 4000-400 cm^{-1} range with a resolution of 4 cm^{-1}. Crystallinity analysis was done via the X-ray diffraction patterns using a Malvern-Panalytical X-ray diffractometer. Samples were analyzed at room temperature with copper radiation ($\lambda = 1.5406$ Å) in the angle of $5 \leq 2\theta^{\circ} \leq 60$ at 45 kV and 40 mA. The textural parameters were obtained from N_2 adsorption-desorption isotherms at -196°C using a Micromeritics ASAP 2020 equipment. These isotherms were analyzed with suitable models to estimate the main textural parameters of these MOFs. Morphology and surface elemental composition of these adsorbents were obtained by scanning electron microscopy (SEM) analysis using a TM3000 (Hitachi) microscope with an energy dispersion system (EDS) (Nano XFlash Bruker).

2.2. Pharmaceutical Adsorption Studies. NAP (≥98%), DFC (≥98%), and APAP (≥99%) were supplied by Sigma-Aldrich and utilized to prepare the adsorbate solutions with deionized water. The main characteristics and molecular structures of these pharmaceuticals are shown in Table 1. Adsorption isotherms of these pharmaceuticals using MIL-100-Fe and MIL-101-Fe MOFs were experimentally quantified at 30–40°C and pH 7. These isotherms were determined with a MOF ratio (W/V) of 10 g/L at batch adsorption

Table 1: Main characteristics of the naproxen, diclofenac, and acetaminophen molecules used as adsorbates in this study.

	Pharmaceutical molecule		
	Acetaminophen	Diclofenac	Naproxen
Chemical structure	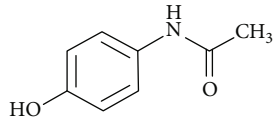	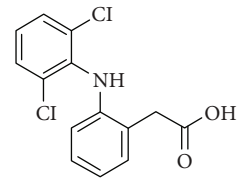	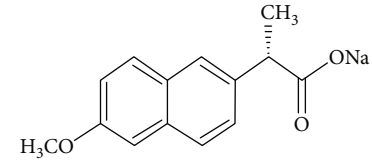
	$C_8H_9NO_2$	$C_{14}H_{11}Cl_2NO_2$	$C_{14}H_{14}O_3$
Molecular weight (g/mol)	151.63	296.15	230.26
Molecular dimension (Å)	$8.56 \times 8.56 \times 1.76$	$7.91 \times 9.58 \times 5.38$	$10.27 \times 6.07 \times 4.59$

conditions under agitation of 120 rpm where the adsorption equilibrium was reached in 24 h. For these experiments, the initial concentrations (C_0) of NAP, DFC, and APAP solutions ranged from 0.157 to 5.292 mmol/L. The pharmaceutical adsorption capacities of tested MOFs (q, mmol/g) were calculated by a mass balance

$$q = \left(\frac{C_0 - C_e}{W}\right)V, \tag{1}$$

where C_e (mmol/L) is the equilibrium concentration of tested pharmaceuticals in the aqueous solution. Concentrations of all pharmaceuticals in the aqueous solutions were quantified by high-performance liquid chromatography (HPLC) (Ultimate 3000TM Thermo Scientific™) at 220 nm with a Thermo Scientific™ Hypersil GOLD™ Aq C18, 3 μm, 4.6 mm × 250 mm reverse-phase HPLC column. A mixture of 0.1% formic acid in water and acetonitrile was the mobile phase with a flow rate of 1 mL/min. The reagents and water used for the mobile phase were HPLC grade. Thermo Scientific™ Chromeleon™ software was utilized to collect and process the pharmaceutical quantification data.

2.3. Thermodynamics and Modeling of the Adsorption of Pharmaceutical Molecules. The thermodynamics of the pharmaceutical adsorption was analyzed calculating the adsorption enthalpy (ΔH°, J/mol) with the van't Hoff approach employing the next equation [27].

$$\ln K_c = \frac{-\Delta H^\circ}{RT} + \frac{\Delta S^\circ}{R}, \tag{2}$$

where R is the universal ideal gas constant (8.3144 J/mol·K), T is the adsorption temperature (K), ΔS° is the adsorption entropy (J/mol·K), and K_c is the adsorption equilibrium constant that was calculated following the procedure reported by Tran et al. [28].

Results of MOF characterization and the analysis of adsorbate molecular structure were utilized to define a statistical-physics-based model to calculate the physicochemical parameters of the adsorption mechanism of pharmaceutical molecules [29–32]. Therefore, this model was utilized to fit the adsorption data and to determine these parameters. It is convenient to note that the adsorption of tested pharmaceutical molecules on these MOFs could imply two surface functionalities: oxygenated functional groups (e.g., -COOH and –OH) and Fe-O clusters. But the complex molecular structure of MOFs limits the possibility of identifying, with reliability, the specific contribution of these functionalities during the pharmaceutical adsorption. Based on these facts, the statistical physic model assumed that one functional group (i.e., oxygenated functionality with or without Fe) was involved in the adsorption of NAP, DFC, and APAP where an adsorbate monolayer was also formed. This model was defined as [33]

$$q_e = \frac{n_{\text{phar}} N_{\text{ads}}}{1 + (C_h/C_e)^{n_{\text{phar}}}}, \tag{3}$$

where n_{phar} represents the number of pharmaceutical molecules adsorbed for each MOF functional group, N_{ads} is the amount of MOF functional groups (mmol/g) involved in the pharmaceutical adsorption, and C_h is the half saturation adsorbate concentration (mmol/L), respectively. The pharmaceutical adsorption capacity at the saturation condition (q_{sat}, mmol/g) of these MOF can be obtained from

$$q_{\text{sat}} = n_{\text{phar}} N_{\text{ads}}. \tag{4}$$

The adsorption energies (ΔE_{ads}, J/mol) related to the molecular interactions between MOF surface and pharmaceutical molecules were calculated using

$$\Delta E_{\text{ads}} = RT \ln\left(\frac{S_{\text{phar}}}{C_h}\right), \tag{5}$$

where S_{phar} is the pharmaceutical solubility (mmol/L) in aqueous solution.

Calculated statistical physics parameters were used to interpret the pharmaceutical adsorption mechanism. They were obtained from the isotherm data correlation via a nonlinear regression where the next objective function (F_{obj}) was minimized

$$F_{\text{obj}} = \sum_{i=1}^{n_{\text{dat}}} \left(q_i^{\text{exp}} - q_i^{\text{mod}}\right)^2, \tag{6}$$

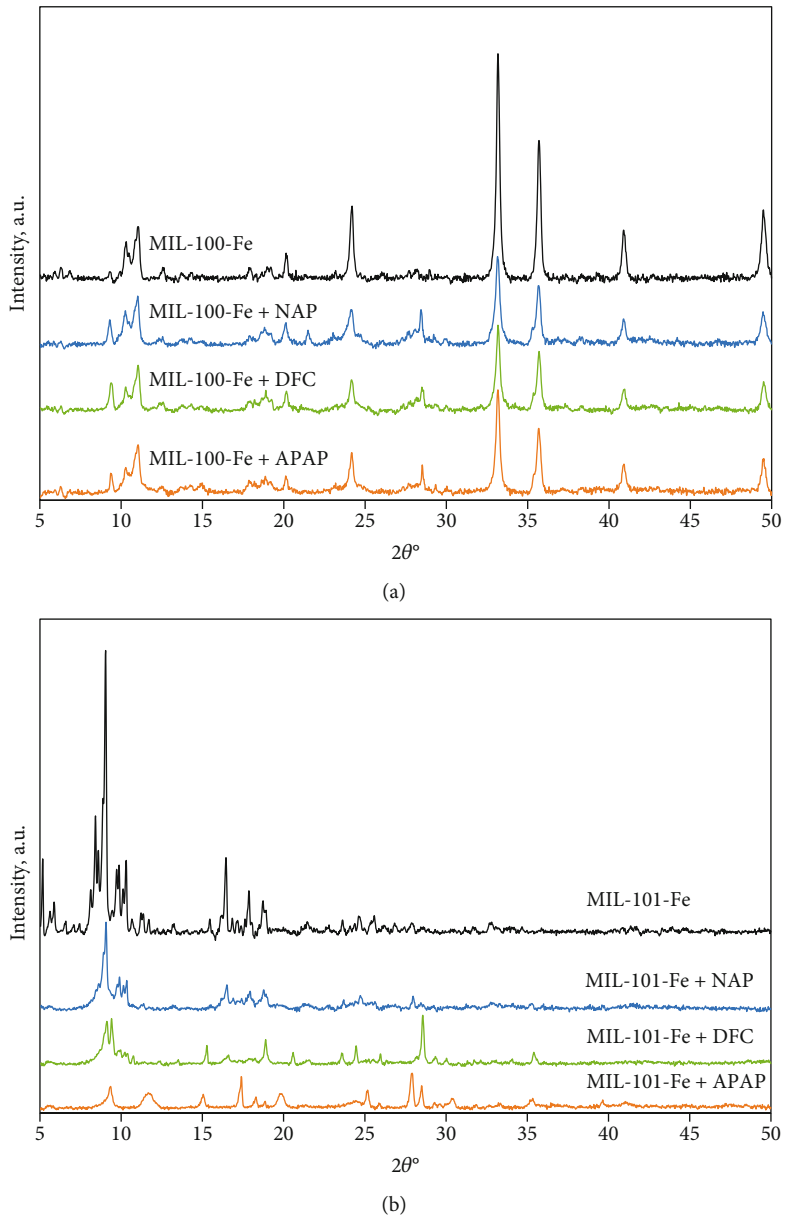

Figure 1: X-ray diffraction patterns of (a) MIL-100-Fe and (b) MIL-101-Fe before and after the adsorption of naproxen (NAP), diclofenac (DFC), and acetaminophen (APAP) molecules.

where exp and mod refer to the experimental and calculated pharmaceutical adsorption capacities, respectively, and n_{dat} is the number of experimental data used in the correlation.

Finally, Density Functional Theory (DFT) calculations were performed with GAUSSIAN09 software to understand the electrostatic and reactive properties of APAP, DFC, and NAP molecules. The molecule optimization was carried out with a functional hybrid B3LYP with 6-311++G(d, p) basis set. The charge distribution of these pharmaceutical molecules was identified with the molecular electrostatic potential (MEP), which was defined as

$$V(r) = \sum_{A} \frac{Z_A}{|R_A - r|} - \int \frac{\rho\left(r'\right) dr'}{|r' - r|}, \tag{7}$$

where $|r' - r|$ is the distance to point r, $\rho(r')dr'$ is the density of the electronic charge (measured as a volume for each element), $|R_A - r|$ is the distance from point r, R_A is the position in space of nucleus A, and Z_A is the atomic number of nucleus A, respectively [34]. Note that in any charge distribution, the electrons and atomic nuclei in molecules generate an electrostatic potential in the space. Therefore, this descriptor provides the electron density response when a unit of positive charge approaches.

3. Results and Discussion

3.1. MOF Characterization. The results of X-ray diffraction of the synthesized MIL-100-Fe and MIL-101-Fe MOFs are reported in Figure 1. X-ray diffractogram of MIL-100-Fe

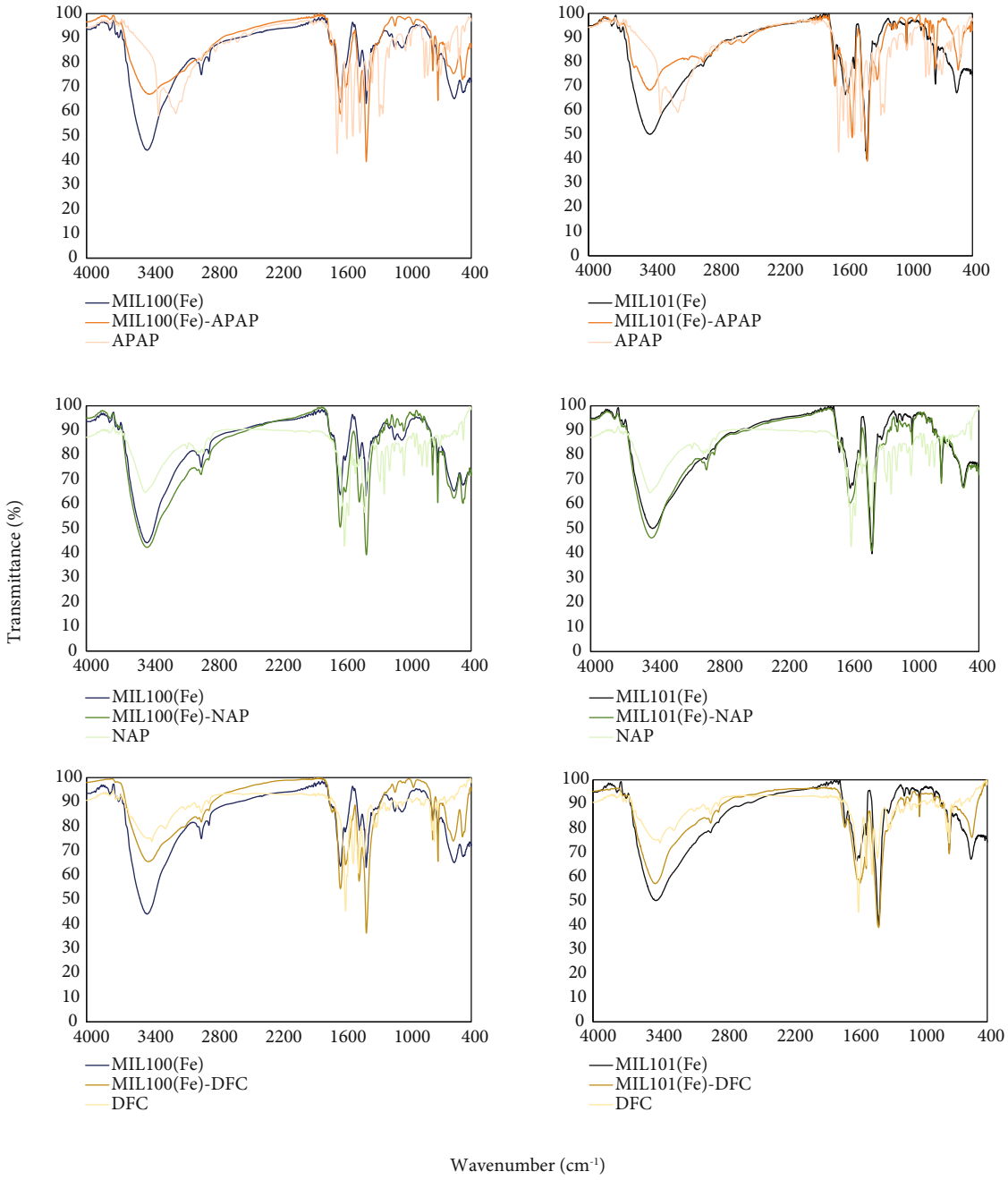

Figure 2: FTIR spectra of (a) MIL-100-Fe and (b) MIL-101-Fe before and after the adsorption of naproxen (NAP), diclofenac (DFC), and acetaminophen (APAP) molecules.

showed the characteristic diffraction peak at ~11.1° 2θ, thus denoting the formation of a pure phase [35, 36]. This result was consistent with those reported by Chen et al. [35], Forghani et al. [36], Pil-Joong et al. [37], Zhang et al. [38], Fan et al. [39], Mahmoodi et al. [40], Nehra et al. [41], Shah et al. [42], Li et al. [43], Chaturvedi et al. [44], Chen et al. [45], and Chávez et al. [46]. After the adsorption of the different pharmaceutical molecules, the MOF crystalline structure was stable but the intensity of the diffraction peaks decreased. These changes in the MOF crystallinity were attributed to incorporation of each adsorbed pharmaceutical on the adsorbent surface [47, 48]. X-ray diffraction pattern of the MIL-101-Fe showed diffraction peaks at ~5.1, 9.2, 16.7, and 19.5° 2θ, which confirmed the formation of the crystalline structure characteristic of this MOF [4, 49–53]. After the adsorption of pharmaceuticals, the X-ray diffraction patterns displayed some changes. Specifically, the disappearance of some diffraction peaks was observed and a change in the MOF crystallinity was also identified. This result could be related to the instability of MOF structure in the aqueous media generated by the incorporation of adsorbed pharmaceuticals on its surface [4, 47].

FTIR spectra of both MOFs are reported in Figure 2. They showed a broad absorption band at 3600–3000 cm^{-1}

Table 2: Elemental analysis and textural parameters of MIL-100-Fe and MIL-101-Fe MOFs.

MOF	Structure	Composition			Pore volume (cm^3/g)		
		Element	Wt%	At%	S_{BET} (m^2/g)	Total	Micropore	Mesopore
MIL-100-Fe	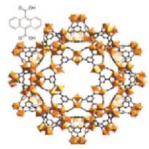	C	52.89	61.75	768.18	0.58	0.31	0.27
		O	42.25	37.03				
		Fe	4.86	1.22				
MIL-101-Fe	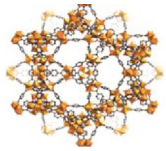	C	50.04	67.98	450.14	1.02	0.19	0.83
		O	23.39	23.85				
		Fe	24.21	7.08				
		Cl	2.37	1.09				

that was attributed to the stretching vibration of the O-H group [35, 36, 40, 41, 43–45, 52, 54, 55]. Iron-based MOFs showed an absorption band at ~1640 cm^{-1} related to the C=O stretching vibration due to carboxyl groups [24, 36, 40, 41, 44, 46, 53, 56]. The spectrum of MIL-100-Fe also displayed the absorption bands of the symmetric (~1425 cm^{-1}) and asymmetric (~1378 cm^{-1}) vibration of the O-C-O group [36, 41, 45], CH bending vibrations (~1112 cm^{-1}) of the carboxylate groups in benzene rings [36, 39, 44], and CH vibrations (~760 and 708 cm^{-1}) of these aromatic structures [46]. FTIR spectrum of MIL-101-Fe showed the absorption bands of asymmetric (~1590 cm^{-1}) and symmetric (1390 cm^{-1}) stretching vibration of the carboxyl groups (O-C=O) present in terephthalic acid, thus indicating the presence of the organic linker (i.e., dicarboxylate) in this sample [49, 51–53]. The absorption band of C-H bending vibration (~746 cm^{-1}) was also identified and corresponded to the aromatic ring of dicarboxylic benzene [49, 52, 53]. Finally, the spectra of these iron-based MOFs also contained the Fe-O stretching vibration at ~550 cm^{-1}, which also agreed with the results of other studies that have reported the synthesis of these MOFs [35, 39, 40, 43, 44, 52, 53].

After the NAP, DFC, and APAP adsorption, FTIR spectra of these MOFs showed a decrement in the intensity of the absorption band associated with the -OH group; see Figure 2. This result suggested the formation of hydrogen bonds between pharmaceutical molecules and MOF surface [57]. Similarly, a change in the absorption band of Fe-O stretching vibration (~550 cm^{-1}) was also observed, which could be an indication that the metal clusters played an important role in the adsorption of these pharmaceuticals [58]. There was also a shift in the absorption band (~1590 cm^{-1}) of the stretching vibration of carboxyl groups (O-C=O) of MIL-101-Fe. According to Tomul et al. [59] and Yaah et al. [60], this change in FTIR spectrum could be also associated with the incorporation of pharmaceutical molecules in the MOF surface. To complement the surface chemistry analysis of adsorbent samples, FTIR spectra of the single pharmaceuticals were also included and compared in Figure 2. Results showed that the specific and characteristic absorption bands of pharmaceutical molecules were also identified in the spectra of MOF samples obtained after the adsorption experiments. Therefore, these findings were an indirect evidence of the adsorption of these molecules on the external surface of these MOFs thus agreeing the results reported in other studies [59, 60].

Table 2 and Figures 3 and 4 show the results obtained from the elemental analysis, SEM images, and textural parameters of tested MOFs. In general, these adsorbents were mainly composed of carbon and oxygen. The presence of iron was confirmed in both MIL-100-Fe (4.9 wt%) and MIL-101-Fe (24.2%) thus providing additional evidence of the successful synthesis of these organometallic structures. Note that chlorine was also identified in the MIL-101-Fe sample because $FeCl_3 \cdot 6H_2O$ was employed as precursor in its synthesis. SEM micrographs of these MOFS indicated that the size of MIL-100-Fe crystals varied from 0.05 to 0.5 μm, while the MIL-101-Fe particles showed an average diameter of 0.5–1 μm; see Figure 3. These results were consistent with other studies [36, 43, 53, 56, 61]. It was also observed that these MOFs presented an octahedral structure; however, the octahedral form of MIL-101-Fe MOF was imperfect [50–52, 62, 63]. N_2 adsorption-desorption isotherms of these MOFs are reported in Figure 4. These N_2 isotherms can be categorized between types I and IV of IUPAC classification, which are typical of micro- and mesoporous materials [23, 37, 41, 43, 52, 53]. The specific surface area, total pore, micropore, and mesopore volumes of these adsorbents are given in Table 2. BET surface area of MIL-100-Fe was 768.18 m^2/g with a total pore volume of 0.58 cm^3/g. This surface area was similar to that reported by Nehra et al. [41] (S_{BET} = 790.5 m^2/g) and Bezverkhyy et al. [64] (S_{BET} = 750 m^2/g). However, the total pore volume differed from that obtained by these authors (i.e., 0.34 and 0.41 cm^3/g). BET surface area and pore volume of MIL-101-Fe were ~450 m^2/g and 1.02 cm^3/g, respectively. Similar textural parameters for this MOF have been reported by Li et al. [49] and Jiang and Li [65]. Herein, it should be noted that the MOF textural parameters depend on the synthesis route because these materials can tune their size by changing the fraction of organic connectivity and the inorganic part, which in turn is associated to the preparation conditions of each organometallic compound.

(a) (b)

Figure 3: SEM micrographs SEM (1000x) of (a) MIL-100-Fe and (b) MIL-101-Fe.

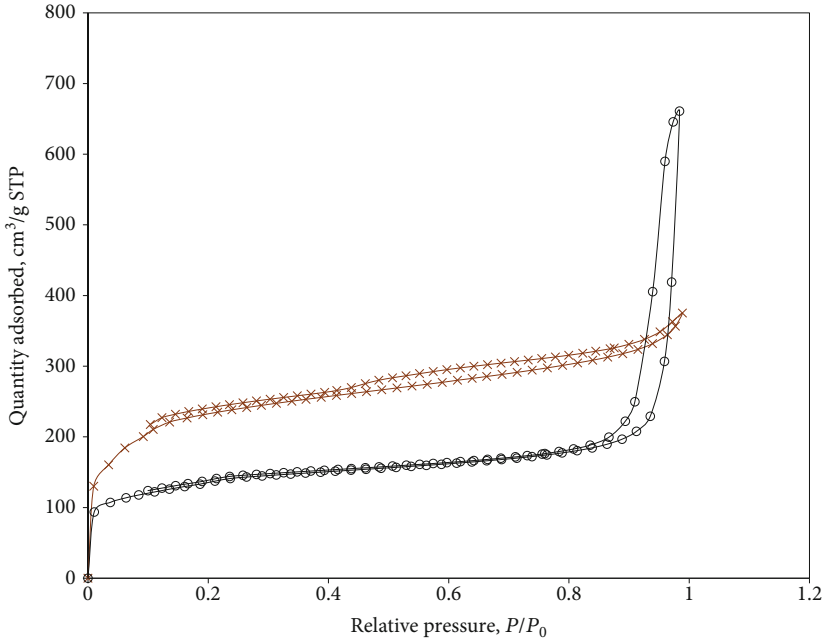

Figure 4: N_2 adsorption-desorption isotherms (at -196°C) of (x) MIL-100-Fe and (○) MIL-101-Fe.

3.2. Adsorption of NAP, DFC, and APAP on MIL-100-Fe and MIL-101-Fe MOFs. Adsorption isotherms of NAP, DFC, and APAP obtained with MIL-100-Fe and MIL-101-Fe MOFs are reported in Figure 5. All pharmaceutical isotherms were 2L type according to the Giles classification for liquid phase adsorption [66], which indicated that the adsorption of these compounds was proportional to the adsorbate concentration until reaching the saturation of the available adsorption sites (i.e., oxygenated functionalities and Fe-O clusters of these MOFs). NAP adsorption capacities of MIL-100-Fe and MIL-101-Fe ranged from 0.186 to 1.267 and 0.205 to 2.190 mmol/g at 30°C and from 0.149 to 1.206 and 0.185 to 1.889 mmol/g at 40°C, respectively. For the case of APAP, the adsorption capacities of these MOFs were 0.012–0.151 and 0.080–0.450 mmol/g at 30°C and 0.009–0.134 and 0.073–0.382 mmol/g at 40°C, respectively. DFC adsorption capacities of MIL-100-Fe varied from 0.182 to 1.708 mmol/g at 30°C and from 0.132 to 1.616 mmol/g at 40°C, while MIL-101-Fe showed DFC adsorption capacities from 0.398 to 1.469 and 0.127 to 1.072 mmol/g at 30 and 40°C, respectively. Table 3 reports and compares the adsorption capacities of MIL-100-Fe, MIL-101-Fe, and other MOFs used in the removal of different pharmaceutical from aqueous solutions [2, 4, 8, 18, 67–69]. Several adsorption capacities reported in the literature were lower than those obtained for NAP, DFC, and APAP with MIL-100-Fe and MIL-101-Fe MOFs. Therefore, these materials could be considered as an alternative separation medium for the adsorption of these three pharmaceuticals in water depollution.

In general, MIL-101-Fe showed a better performance than MIL-100-Fe for the adsorption of NAP and APAP, while the highest DFC adsorption capacities were obtained with MIL-100-Fe. The pharmaceutical adsorption capacities of MIL-100-Fe and MIL-101-Fe followed the next trends: APAP < <NAP < DFC and APAP < <DFC < NAP,

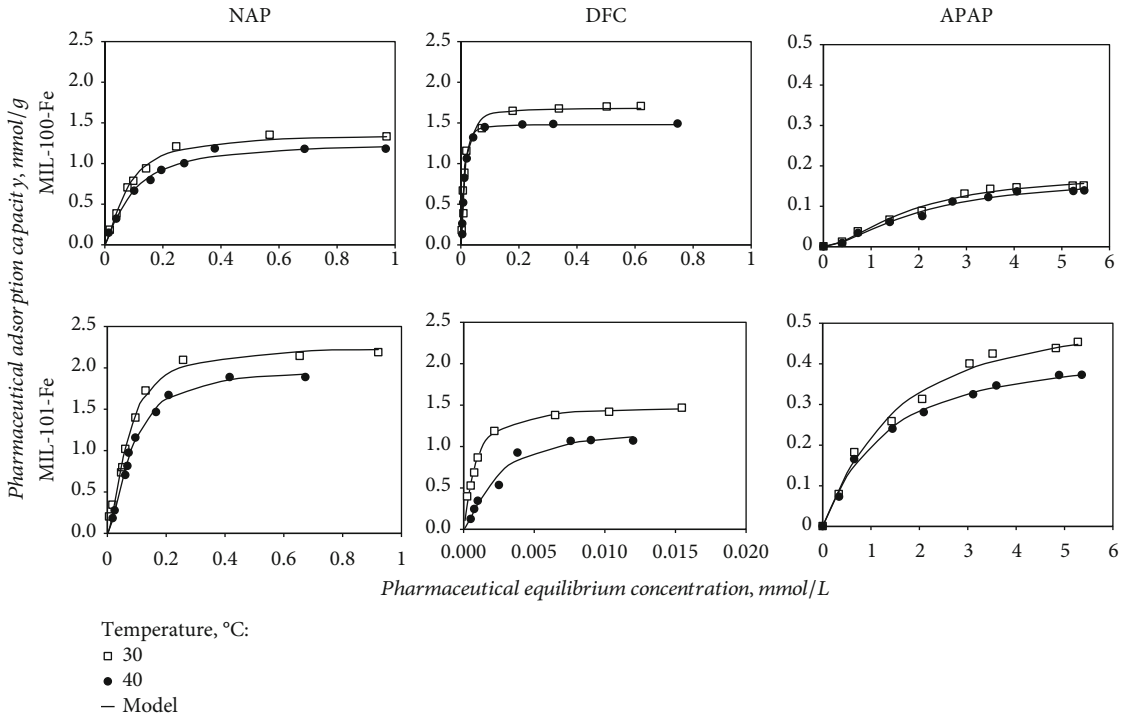

Figure 5: Isotherms of the adsorption of the adsorption of acetaminophen, diclofenac, and naproxen on MIL-100-Fe and MIL-101-Fe from aqueous solution at pH 7.

Table 3: Adsorption capacities for different pharmaceuticals using MOFs as adsorbents.

MOF	Adsorbate	Experimental conditions		Adsorption capacity (mmol/g)	Reference
		pH	Temperature (°C)		
MIL-100-Fe	Naproxen	4.5	25	0.499	Hasan et al. [2]
UiO-66		5.4	25	0.638	
NH2-UiO-66	Diclofenac			0.358	Hasan et al. [18]
18%SO_3H-UiO-66				0.881	
	Sulfamethoxazole	4.9	25	0.343	Ahmed [8]
ZIF-8	Ibuprofen	5	25	0.673	Bhadra et al. [69]
	Diclofenac			0.354	
MIL-101-Cr	Naproxen	7	25	0.429	Sarker et al. [68]
	Ketoprofen			0.259	
MIL-101-Cr (Gno)	Naproxen	7	25	0.538	
	Ketoprofen			0.361	
Fe_3O_4@MIL-100-Fe	Diclofenac	6.2	25	1.351	Li et al. [67]
MIL-100-Fe	Tetracycline	7	25	0.851	Dong et al. [4]
	Acetaminophen	7	30	0.143	This study
MIL-100-Fe	Diclofenac			1.542	
	Naproxen			1.354	
	Acetaminophen	7	30	0.423	
MIL-101-Fe	Diclofenac			1.760	
	Naproxen			1.730	

respectively. It was clear that these adsorption capacities depended on both MOF and pharmaceutical properties. As stated, BET surface area of MIL-100-Fe was higher than that of MIL-101-Fe. For both MOFs, it was expected that the pharmaceutical adsorption was performed mainly on the external adsorbent surface due to the size of these organic molecules. However, the volume of mesopores of MIL-100-Fe was lower than that of MIL-100-Fe; see

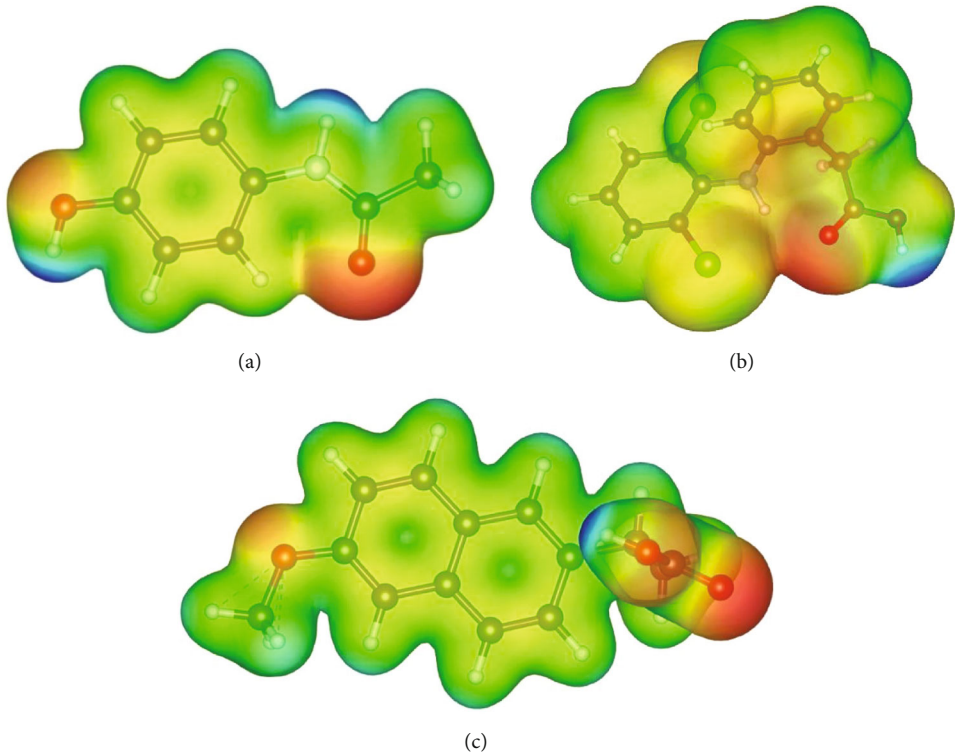

Figure 6: Molecular electrostatic potential of (a) acetaminophen, (b) diclofenac, and (c) naproxen molecules.

Table 2. These results suggested that the adsorption of these pharmaceutical molecules was favored by large pores in MOF structure. Also, the contribution of Fe-O clusters on these MOFs played a relevant role in the adsorption of APAP and NAP pharmaceuticals where the adsorbent with the highest Fe content (i.e., MIL-101-Fe) also showed the highest removal.

The solution temperature affected the pharmaceutical adsorption with these MOFs; see Figure 5. All the maximum adsorption capacities ranged from 0.14 to 2.19 mmol/g and decreased in 7.9–27% when the solution temperature increased from 30 to 40°C. Pharmaceutical adsorption on both MOFs was affected by the solution temperature according to the next trend: NAP < APAP < DFC. In particular, the removal performance of MIL-101-Fe was more sensitive to the solution temperature where its pharmaceutical adsorption capacities reduced from 13.7% for NAP to 27% for DFC. This exothermic adsorption was partially associated to the solubility of these pharmaceuticals in water and the energy exchange that occurred during the separation process [70]. Specifically, the solubility of these pharmaceutical molecules increased with the solution temperature thus affecting the intermolecular attractive forces between the MOF structure and these adsorbates [4, 70]. Calculated enthalpies for the exothermic adsorption of tested pharmaceuticals on these MOFs ranged from 19.1 to 65.1 kJ/mol. These enthalpy values could correspond to an adsorption caused by hydrogen bonds, van der Waals forces, and electrostatic interactions [71–73].

With respect to the pharmaceutical molecular properties, the literature indicates that the molecular weight and hydrophobicity of these organic compounds could impact their adsorption on MOFs [6, 8]. Figure 6 shows the MEPs of NAP, APAP, and DFC molecules that were calculated with DFT. These electrostatic potentials are illustrated via a color mapping where the scale indicates from the most reactive to the least reactive zone of the molecule (i.e., red > orange > yellow > green > blue). APAP molecule had negative charges located on the oxygen atoms, which were identified in the hydroxyl group in the para position and the oxygen of the acetate. This pharmaceutical molecule had two positive charges located on the hydrogen atoms of the secondary amine and on the hydrogen atom located in the -OH group in the para position. The remaining of this molecule showed a behavior mainly oriented towards the repulsion, which was identified by its green color [74, 75]. DFC molecule showed a high chemical reactivity where the area of interest of this adsorbate corresponded to the -COOH group. The molecular area of least reactivity (blue color) was identified in the hydroxyl group of the carboxyl (mainly in the H atom), and the most reactive area (red color) was found on the oxygen atom attached to the carbon from the carboxyl group. The rest of this molecule showed an intermediate reactivity (i.e., yellow zones) [76, 77]. Finally, the highest reactivity zone of NAP molecule was the oxygen of the methoxyl and -COOH groups, while the less reactivity zone was identified in the hydrogen of the -COOH group. The rest of this pharmaceutical molecule had a low reactivity [78, 79]. DFT calculations also supported that the more reactive zones of these pharmaceuticals molecules could interact mainly with Fe-O clusters on MOF structure during the adsorption.

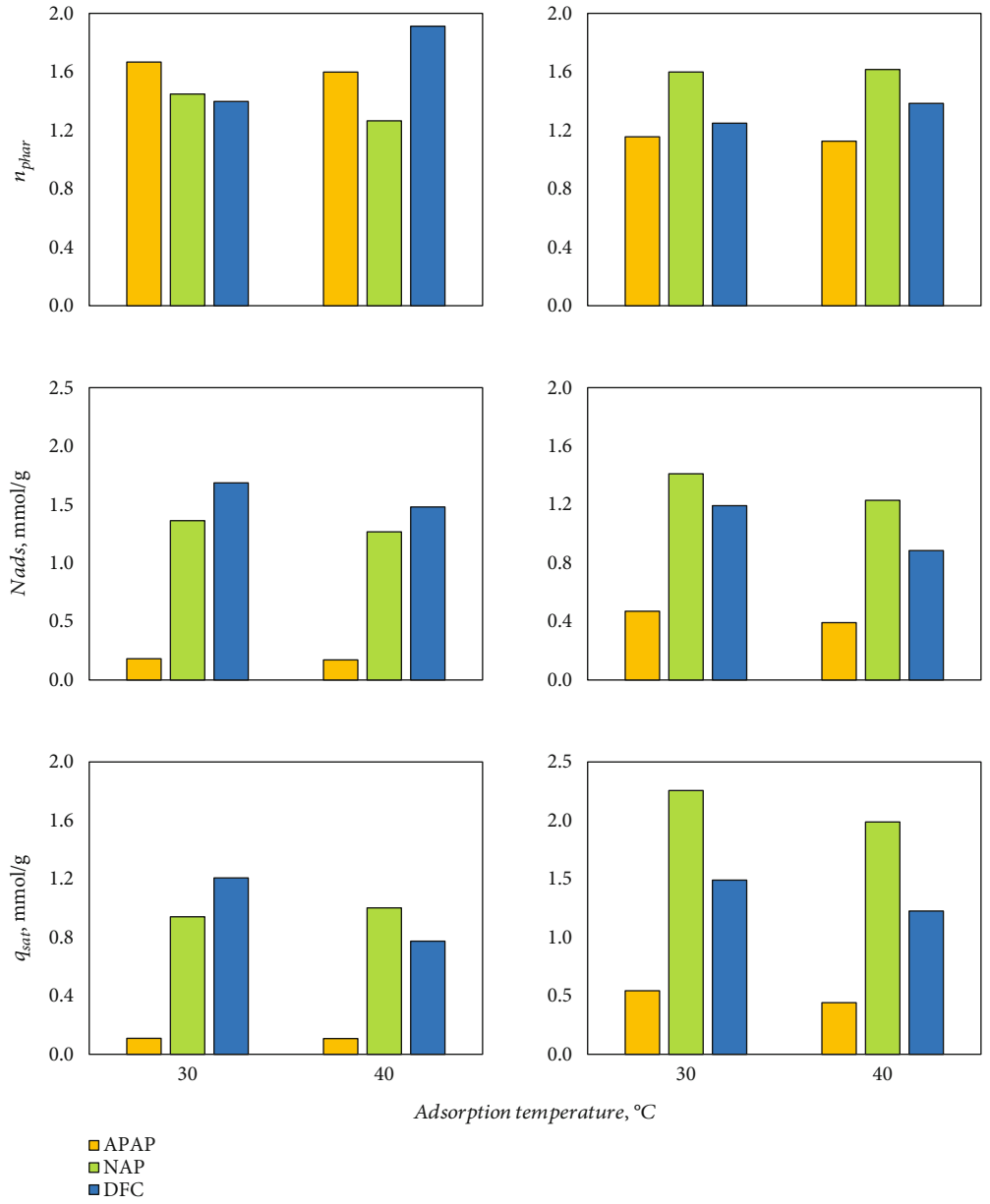

Figure 7: Calculated physicochemical parameters of the adsorption of acetaminophen, diclofenac, and naproxen on MIL-100-Fe and MIL-101-Fe from aqueous solution at pH 7.

Calculated physicochemical parameters for the adsorption of these pharmaceuticals on MIL-100-Fe and MIL-101-Fe MOFs are reported in Figure 7. This statistical physics model showed $R^2 \geq 0.97$ for all pharmaceutical isotherms. Modeling results indicated that the number of pharmaceutical molecules adsorbed per functional groups of MIL-100-Fe and MIL-101-Fe ranged from 1.3 to 1.9 and 1.1 to 1.6, respectively. A multimolecular adsorption of these pharmaceuticals occurred in both MOFs especially for MIL-101-Fe. As stated, MIL-101-Fe showed the highest Fe content and it could be expected that its Fe-O clusters could interact simultaneously with more than one pharmaceutical molecule during the adsorption. N_{ads} ranged from 0.1 to 1.2 mmol/g for MIL-100-Fe and from 0.4 to 1.4 mmol/g for MIL-101-Fe, respectively. The increment of adsorption temperature reduced the number of functional groups involved in the pharmaceutical adsorption due to some adsorbate–functional group interactions were broken caused by the thermal agitation effect [33]. The saturation adsorption capacities were 0.17–1.69 mmol/g for MIL-100-Fe and 0.44–2.26 mmol/g for MIL-101-Fe. The lowest adsorption capacities at saturation were obtained for APAP with both MOFs. In particular, MIL-100-Fe showed the highest saturation adsorption capacities for DFC, while MIL-101-Fe had the highest saturation adsorption capacities for NAP. Calculated adsorption interaction energies were 10.6–22.6 kJ/mol for MIL-100-Fe and 11.4–28.6 kJ/mol for MIL-101-Fe. These pharmaceutical-MOF interaction energies were consistent with the calculated adsorption entropies thus confirming that hydrogen bonds,

van der Waals forces, and electrostatic interactions could be present in the adsorption mechanism of these organic molecules.

4. Conclusions

The adsorption of three relevant pharmaceuticals on MIL-100-Fe and MIL-101-Fe MOFs from aqueous solutions has been experimentally studied and modeled to understand their adsorption mechanism. Results showed that the pharmaceutical adsorption capacities of these MOFs were mainly related to the presence of Fe-O clusters where their mesopore structure contributed for the removal of these organic pollutants. Adsorption properties of MIL-101-Fe outperformed those obtained for MIL-100-Fe. Overall, both MOFs showed the lowest adsorption capacities for acetaminophen molecules. The adsorption of naproxen, diclofenac, and acetaminophen on these MOFs was a multimolecular and exothermic process where more than one pharmaceutical molecule can interact with one functional group from the adsorbent surface. The pharmaceutical adsorption properties of MIL-101-Fe MOF were more sensitive to increments of solution temperature and decreased up to 27% for diclofenac molecules. MOF characterization, DFT, and statistical physics calculations indicated that hydrogen bonds, van der Waals and electrostatic forces could be the main interactions involved in the pharmaceutical adsorption on tested MOFs. MIL-101-Fe is an interesting material with better pharmaceutical adsorption capacities than other MOFs reported in literature, and it can be utilized to prepare composites and other materials for water depollution. Therefore, the experimental and theoretical results reported in this study can contribute to enhance and consolidate the application of MOFs as adsorbents of emerging compounds for water treatment and purification.

Data Availability

Data of this paper are available on request to the corresponding author.

Conflicts of Interest

The authors declared no potential conflicts of interest with respect to the research, authorship, and/or publication of this article.

Acknowledgments

The authors acknowledge the financial support provided by CONACYT (Grant No. A1-S-10035) for the present study.

References

[1] C. Peña-Guzmán, S. Ulloa-Sánchez, K. Mora et al., "Emerging pollutants in the urban water cycle in Latin America: a review of the current literature," *Journal of Environmental Management*, vol. 237, pp. 408–423, 2019.

[2] Z. Hasan, J. Jeon, and S. H. Jhung, "Adsorptive removal of naproxen and clofibric acid from water using metal- organic frameworks," *Journal of Hazardous Materials*, vol. 209-210, pp. 151–157, 2012.

[3] L. Zhu, L. Meng, J. Shi, J. Li, X. Zhang, and M. Feng, "Metal-organic frameworks/carbon-based materials for environmental remediation: a state-of-the-art mini-review," *Journal of Environmental Management*, vol. 232, pp. 964–977, 2019.

[4] Y. Dong, T. Hu, M. Pudukudy et al., "Influence of microwave-assisted synthesis on the structural and textural properties of mesoporous MIL-101(Fe) and NH_2-MIL-101(Fe) for enhanced tetracycline adsorption," *Materials Chemistry and Physics*, vol. 251, article 123060, 2020.

[5] Z. Hasan, N. A. Khan, and S. H. Jhung, "Adsorptive purification of organic contaminants of emerging concern from water with metal-organic frameworks," *Contaminants of Emerging Concern in Water and Wastewater*, pp. 47–92, 2020.

[6] C. Jung, L. K. Boateng, J. R. V. Flora et al., "Competitive adsorption of selected non-steroidal anti-inflammatory drugs on activated biochars: experimental and molecular modeling study," *Chemical Engineering Journal*, vol. 264, pp. 1–9, 2015.

[7] M. Parolini, "Toxicity of the non-steroidal anti-inflammatory drugs (NSAIDs) acetylsalicylic acid, paracetamol, diclofenac, ibuprofen and naproxen towards freshwater invertebrates: a review," *Science of the Total Environment*, vol. 740, article 140043, 2020.

[8] M. J. Ahmed, "Adsorption of non-steroidal anti-inflammatory drugs from aqueous solution using activated carbons: review," *Journal of Environmental Management*, vol. 190, pp. 274–282, 2017.

[9] A. Gómez-Avilés, L. Sellaoui, M. Badawi, A. Bonilla-Petriciolet, J. Bedia, and C. Belver, "Simultaneous adsorption of acetaminophen, diclofenac and tetracycline by organo-sepiolite: experiments and statistical physics modelling," *Chemical Engineering Journal*, vol. 404, article 126601, 2021.

[10] D. A. G. Sumalinog, S. C. Capareda, and M. D. G. de Luna, "Evaluation of the effectiveness and mechanisms of acetaminophen and methylene blue dye adsorption on activated biochar derived from municipal solid wastes," *Journal of Environmental Management*, vol. 210, pp. 255–262, 2018.

[11] L. A. Al-Khateeb, W. Hakami, and M. A. Salam, "Removal of non-steroidal anti-inflammatory drugs from water using high surface area nanographene: kinetic and thermodynamic studies," *Journal of Molecular Liquids*, vol. 241, pp. 733–741, 2017.

[12] K. Vargas-Berrones, L. Bernal-Jácome, L. D. de León-Martínez, and R. Flores-Ramírez, "Emerging pollutants (EPs) in Latin America: a critical review of under-studied EPs, case of study -nonylphenol-," *Science of the Total Environment*, vol. 726, article 138493, 2020.

[13] C. R. Gadipelly, K. V. Marathe, and V. K. Rathod, "Effective adsorption of ciprofloxacin hydrochloride from aqueous solutions using metal-organic framework," *Separation Science and Technology*, vol. 53, no. 17, pp. 2826–2832, 2018.

[14] H. T. M. Thanh, T. T. T. Phuong, P. T. L. Hang et al., "Comparative study of Pb(II) adsorption onto MIL-101 and Fe-MIL-101 from aqueous solutions," *Journal of Environmental Chemical Engineering*, vol. 6, no. 4, pp. 4093–4102, 2018.

[15] G. Sharma, V. K. Gupta, S. Agarwal et al., "Fabrication and characterization of trimetallic nano-photocatalyst for remediation of ampicillin antibiotic," *Journal of Molecular Liquids*, vol. 260, pp. 342–350, 2018.

[16] A. Kumar, S. K. Sharma, G. Sharma et al., "Silicate glass $_2$O/$Cu_2V_2O_7$ p-n heterojunction for enhanced

visible light photo-degradation of sulfamethoxazole: high charge separation and interfacial transfer," *Journal of Hazardous Materials*, vol. 402, article 123790, 2021.

[17] M. G. Orcajo, J. A. Botas, G. Calleja, and M. Sánchez-Sánchez, "Materiales MOF para el almacenamiento de hidrógeno," *Real Sociedad Española de Química*, vol. 108, no. 1, pp. 13–20, 2012.

[18] Z. Hasan, N. A. Khan, and S. H. Jhung, "Adsorptive removal of diclofenac sodium from water with Zr-based metal-organic frameworks," *Chemical Engineering Journal*, vol. 284, pp. 1406–1413, 2016.

[19] S. Dhaka, R. Kumar, A. Deep, M. B. Kurade, S. W. Ji, and B. H. Jeon, "Metal-organic frameworks (MOFs) for the removal of emerging contaminants from aquatic environments," *Coordination Chemistry Reviews*, vol. 380, pp. 330–352, 2019.

[20] A. Samokhvalov, "Adsorption on mesoporous metal–organic frameworks in solution: aromatic and heterocyclic compounds," *European Journal*, vol. 21, no. 47, pp. 16726–16742, 2015.

[21] D. Sompornpailin, C. Ratanatawanate, C. Sattayanon, S. Namuangruk, and P. Punyapalakul, "Selective adsorption mechanisms of pharmaceuticals on benzene-1,4-dicarboxylic acid-based MOFs: effects of a flexible framework, adsorptive interactions and the DFT study," *Science of the Total Environment*, vol. 720, article 137449, 2020.

[22] K. Ah-Reum, Y. Tae-Ung, K. Eun-Jung et al., "Facile loading of Cu(I) in MIL-100(Fe) through redox-active Fe(II) sites and remarkable propylene/propane separation performance," *Chemical Engineering Journal*, vol. 331, pp. 777–784, 2018.

[23] F. Tan, M. Liu, K. Li et al., "Facile synthesis of size-controlled MIL-100(Fe) with excellent adsorption capacity for methylene blue," *Chemical Engineering Journal*, vol. 281, pp. 360–367, 2015.

[24] R. Zhou, J. Yu, and R. Chi, "Selective removal of phosphate from aqueous solution by MIL-101(Fe)/bagasse composite prepared through bagasse size control," *Environmental Research*, vol. 188, article 109817, 2020.

[25] Y. Pi, X. Li, Q. Xia et al., "Adsorptive and photocatalytic removal of persistent organic pollutants (POPs) in water by metal-organic frameworks (MOFs)," *Chemical Engineering Journal*, vol. 337, pp. 351–371, 2018.

[26] Z. Abbasi, L. Cseri, X. Zhang, B. P. Ladewig, and H. Wang, "Metal–organic frameworks (MOFs) and MOF-derived porous carbon materials for sustainable adsorptive wastewater treatment," in *Sustainable Nanoscale Engineering*, pp. 163–194, Elsevier, 2020.

[27] H. V. Tran, L. T. Hoang, and C. D. Huynh, "An investigation on kinetic and thermodynamic parameters of methylene blue adsorption onto graphene-based nanocomposite," *Chemical Physics*, vol. 535, article 110793, 2020.

[28] H. N. Tran, S. J. You, A. Hosseini-Bandegharaei, and H. P. Chao, "Mistakes and inconsistencies regarding adsorption of contaminants from aqueous solutions: a critical review," *Water Research*, vol. 120, pp. 88–116, 2017.

[29] X. Pang, L. Sellaoui, D. Franco et al., "Adsorption of crystal violet on biomasses from pecan nutshell, para chestnut husk, araucaria bark and palm cactus: experimental study and theoretical modeling via monolayer and double layer statistical physics models," *Chemical Engineering Journal*, vol. 378, article 122101, 2019.

[30] Z. Li, L. Sellaoui, D. Franco et al., "Adsorption of hazardous dyes on functionalized multiwalled carbon nanotubes in single and binary systems: experimental study and physicochemical interpretation of the adsorption mechanism," *Chemical Engineering Journal*, vol. 389, article 124467, 2020.

[31] G. L. Dotto, M. L. G. Vieria, J. O. Goncalves, and P. L. A. de Almeida, "Remoção dos corantes azul brilhante, amarelo crepúsculo e amarelo tartrazina de soluções aquosas utilizando carvão ativado, terra ativada, terra diatomácea, quitina e quitosana: estudos de equilíbrio e termodinâmica," *Quimica Nova*, vol. 34, no. 7, pp. 1193–1199, 2011.

[32] B. S. Marques, T. S. Frantz, T. R. S. A. Cadaval Jr, L. A. de Almeida Pinto, and G. L. Dotto, "Adsorption of a textile dye onto piaçava fibers: kinetic, equilibrium, thermodynamics, and application in simulated effluents," *Pollution Research*, vol. 26, no. 28, pp. 28584–28592, 2019.

[33] O. Amrhar, L. El Gana, and M. Mobarak, "Calculation of adsorption isotherms by statistical physics models: a review," *Environmental Chemistry Letters*, vol. 19, no. 6, pp. 4519–4547, 2021.

[34] V. J. Landin-Sandoval, D. I. Mendoza-Castillo, M. K. Seliem et al., "Physicochemical analysis of multilayer adsorption mechanism of anionic dyes on lignocellulosic biomasses via statistical physics and density functional theory," *Journal of Molecular Liquids*, vol. 322, article 114511, 2021.

[35] S. Chen, K. Wen, X. Zhang, R. Zhang, and R. Han, "Adsorption of neutral red onto MIL-100(Fe) from solution: characterization, equilibrium, kinetics, thermodynamics and process design," *Desalination and Water Treatment*, vol. 177, pp. 197–208, 2020.

[36] M. Forghani, A. Azizi, M. J. Livani, and L. A. Kafshgari, "Adsorption of lead(II) and chromium(VI) from aqueous environment onto metal- organic framework MIL-100(Fe): synthesis, kinetics, equilibrium and thermodynamics," *Journal of Solid State Chemistry*, vol. 291, article 121636, 2020.

[37] K. Pil-Joong, Y. Young-Woo, P. Hosik et al., "Separation of SF_6 from SF_6/N_2 mixture using metal-organic framework MIL-100(Fe) granule," *Chemical Engineering Journal*, vol. 262, pp. 683–690, 2015.

[38] F. Zhang, Y. Jin, J. Shi, Y. Zhong, W. Zhu, and M. S. El-Shall, "Polyoxometalates confined in the mesoporous cages of metal-organic framework MIL-100(Fe): efficient heterogeneous catalysts for esterification and acetalization reactions," *Chemical Engineering Journal*, vol. 269, pp. 236–244, 2015.

[39] J. Fan, D. Chen, N. Li et al., "Adsorption and biodegradation of dye in wastewater with Fe_3O_4@MIL-100 (Fe) core-shell bionanocomposites," *Chemosphere*, vol. 191, pp. 315–323, 2018.

[40] N. M. Mahmoodi, J. Abdi, M. Oveisi, A. M. Asli, and M. Vossoughi, "Metal-organic framework (MIL-100 (Fe)): synthesis, detailed photocatalytic dye degradation ability in colored textile wastewater and recycling," *Materials Research Bulletin*, vol. 100, pp. 357–366, 2018.

[41] M. Nehra, N. Dilbaghi, N. K. Singhal, A. A. Hassan, K. H. Kim, and S. Kumar, "Metal organic frameworks MIL-100(Fe) as an efficient adsorptive material for phosphate management," *Environmental Research*, vol. 169, pp. 229–236, 2019.

[42] W. A. Shah, L. Noureen, M. A. Nadeem, and P. Kögerler, "Encapsulation of keggin-type manganese-polyoxomolybdates in MIL-100 (Fe) for efficient reduction of p-nitrophenol," *Journal of Solid State Chemistry*, vol. 268, pp. 75–82, 2018.

[43] H. Li, F. Liu, X. Ma et al., "Catalytic performance of strontium oxide supported by MIL-100(Fe) derivate as transesterification

catalyst for biodiesel production," *Energy Conversion and Management*, vol. 180, pp. 401–410, 2019.

[44] G. Chaturvedi, A. Kaur, A. Umar, M. A. Khan, H. Algarni, and S. K. Kansal, "Removal of fluoroquinolone drug, levofloxacin, from aqueous phase over iron based MOFs, MIL-100(Fe)," *Journal of Solid State Chemistry*, vol. 281, article 121029, 2020.

[45] T. Chen, T. Da, and Y. Ma, "Reasonable calculation of the thermodynamic parameters from adsorption equilibrium constant," *Journal of Molecular Liquids*, vol. 322, article 114980, 2021.

[46] A. M. Chávez, A. Rey, J. López, P. M. Álvarez, and F. J. Beltrán, "Critical aspects of the stability and catalytic activity of MIL-100(Fe) in different advanced oxidation processes," *Separation and Purification Technology*, vol. 255, article 117660, 2021.

[47] L. Zhao, M. R. Azhar, X. Li et al., "Adsorption of cerium (III) by HKUST-1 metal-organic framework from aqueous solution," *Journal of Colloid and Interface Science*, vol. 542, pp. 421–428, 2019.

[48] B. Anand, S. A. Younis, J. E. Szulejko, K. H. Kim, and W. Zhang, "The potential utility of HKUST-1 for adsorptive removal of benzene vapor from gaseous streams using a denuder versus a packed-bed adsorption system," *Journal of Cleaner Production*, vol. 275, article 122359, 2020.

[49] Z. Li, X. Liu, W. Jin, Q. Hu, and Y. Zhao, "Adsorption behavior of arsenicals on MIL-101(Fe): the role of arsenic chemical structures," *Journal of Colloid and Interface Science*, vol. 554, pp. 692–704, 2019.

[50] X. Q. Tang, Y. D. Zhang, Z. W. Jiang, D. M. Wang, C. Z. Huang, and Y. F. Li, "Fe_3O_4 and metal-organic framework MIL-101(Fe) composites catalyze luminol chemiluminescence for sensitively sensing hydrogen peroxide and glucose," *Talanta*, vol. 179, pp. 43–50, 2018.

[51] H. Fakhri, M. Farzadkia, R. Boukherroub, V. Srivastava, and M. Sillanpää, "Design and preparation of core-shell structured magnetic graphene (Fe): photocatalysis under shell to remove diazinon and atrazine pesticides," *Solar Energy*, vol. 208, pp. 990–1000, 2020.

[52] A. Jarrah and S. Farhadi, "Encapsulation of $K_6P_2W_{18}O_{62}$ into magnetic nanoporous Fe_3O_4/MIL-101 (Fe) for highly enhanced removal of organic dyes," *Journal of Solid State Chemistry*, vol. 285, article 121264, 2020.

[53] Z. Zhang, Y. Chen, Z. Wang et al., "Effective and structure-controlled adsorption of tetracycline hydrochloride from aqueous solution by using Fe-based metal-organic frameworks," *Applied Surface Science*, vol. 542, article 148662, 2021.

[54] G. I. Dzhardimalieva, R. K. Baimuratova, E. I. Knerelman et al., "Synthesis of copper(II) trimesinate coordination polymer and its use as a sorbent for organic dyes and a precursor for nanostructured material," *Polymers*, vol. 12, no. 5, p. 1024, 2020.

[55] M. Mohammadnejad and M. Fakhrefatemi, "Synthesis of magnetic HKUST-1 metal-organic framework for efficient removal of mefenamic acid from water," *Journal of Molecular Structure*, vol. 1224, article 129041, 2021.

[56] H. Y. Jang, J. K. Kang, J. A. Park, S. C. Lee, and S. B. Kim, "Metal-organic framework MIL-100(Fe) for dye removal in aqueous solutions: prediction by artificial neural network and response surface methodology modeling," *Environmental Pollution*, vol. 267, article 115583, 2020.

[57] D. T. Nguyen, H. N. Tran, R. S. Juang et al., "Adsorption process and mechanism of acetaminophen onto commercial activated carbon," *Journal of Environmental Chemical Engineering*, vol. 8, no. 6, article 104408, 2020.

[58] H. E. Reynel-Avila, D. I. Mendoza-Castillo, A. Bonilla-Petriciolet, and J. Silvestre-Albero, "Assessment of naproxen adsorption on bone char in aqueous solutions using batch and fixed-bed processes," *Journal of Molecular Liquids*, vol. 209, pp. 187–195, 2015.

[59] F. Tomul, Y. Arslan, B. Kabak, D. Trak, and H. N. Tran, "Adsorption process of naproxen onto peanut shell-derived biosorbent: important role of n–π interaction and van der Waals force," *Journal of Chemical Technology & Biotechnology*, vol. 96, no. 4, pp. 869–880, 2021.

[60] K. V. B. Yaah, M. Zbair, B. de Oliveira, and S. Ojala, "Hydrochar-derived adsorbent for the removal of diclofenac from aqueous solution," *Nanotechnology for Environmental Engineering*, vol. 6, no. 1, pp. 2–12, 2021.

[61] P. B. So, H. T. Chen, and C. H. Lin, "*De novo* synthesis and particle size control of iron metal organic framework for diclofenac drug delivery," *Microporous and Mesoporous Materials*, vol. 309, article 110495, 2020.

[62] P. D. Du, H. T. M. Thanh, T. C. To et al., "Metal-organic framework MIL-101: synthesis and photocatalytic degradation of remazol black B dye," *Journal of Nanomaterials*, vol. 2019, Article ID 6061275, 15 pages, 2019.

[63] A. Hamedi, M. B. Zarandi, and M. R. Nateghi, "Highly efficient removal of dye pollutants by MIL-101(Fe) metal-organic framework loaded magnetic particles mediated by poly L-Dopa," *Journal of Environmental Chemical Engineering*, vol. 7, no. 1, article 102882, 2019.

[64] I. Bezverkhyy, G. Weber, and J. P. Bellat, "Degradation of fluoride-free MIL-100(Fe) and MIL-53(Fe) in water: effect of temperature and pH," *Microporous and Mesoporous Materials*, vol. 219, pp. 117–124, 2016.

[65] Z. Jiang and Y. Li, "Facile synthesis of magnetic hybrid Fe_3O_4/MIL-101 via heterogeneous coprecipitation assembly for efficient adsorption of anionic dyes," *Journal of the Taiwan Institute of Chemical Engineers*, vol. 59, pp. 373–379, 2016.

[66] C. H. Giles, T. H. MacEwan, S. N. Nakhwa, and D. Smith, "Studies in adsorption. Part XI. A system of classification of solution adsorption isotherms, and its use in diagnosis of adsorption mechanisms and in measurement of specific surface areas of solids," *Journal of the Chemical Society*, vol. 111, pp. 3973–3993, 1960.

[67] S. Li, J. Cui, X. Wu, X. Zhang, and X. Hou, "Rapid in situ microwave synthesis of Fe_3O_4@MIL-100(Fe) for aqueous diclofenac sodium removal through integrated adsorption and photodegradation," *Journal of Hazardous Materials*, vol. 373, pp. 408–416, 2019.

[68] M. Sarker, J. Y. Song, and S. H. Jhung, "Adsorptive removal of anti-inflammatory drugs from water using graphene oxide/metal-organic framework composites," *Chemical Engineering Journal*, vol. 335, pp. 74–81, 2018.

[69] B. N. Bhadra, A. Vinu, C. Serre, and S. H. Jhung, "MOF-derived carbonaceous materials enriched with nitrogen: preparation and applications in adsorption and catalysis," *Materials Today*, vol. 25, pp. 88–111, 2019.

[70] E. M. Cuerda-Correa, J. R. Domínguez-Vargas, F. J. Olivares-Marín, and J. B. de Heredia, "On the use of carbon blacks as potential low-cost adsorbents for the removal of non-steroidal anti-inflammatory drugs from river water," *Journal of Hazardous Materials*, vol. 177, no. 1-3, pp. 1046–1053, 2010.

[71] S. Jodeh, F. Abdelwahab, N. Jaradat, I. Warad, and W. Jodeh, "Adsorption of diclofenac from aqueous solution using Cyclamen persicum tubers based activated carbon (CTAC)," *Journal of the Association of Arab Universities for Basic and Applied Sciences*, vol. 20, no. 1, pp. 32–38, 2016.

[72] S. Raghav and D. Kumar, "Adsorption equilibrium, kinetics, and thermodynamic studies of fluoride adsorbed by tetrametallic oxide adsorbent," *Journal of Chemical & Engineering*, vol. 63, no. 5, pp. 1682–1697, 2018.

[73] S. Lombardo and W. Thielemans, "Thermodynamics of adsorption on nanocellulose surfaces," *Cellulose*, vol. 26, no. 1, pp. 249–279, 2019.

[74] K. A. Ford, "Role of electrostatic potential in the in silico prediction of molecular bioactivation and mutagenesis," *Molecular Pharmaceutics*, vol. 10, no. 4, pp. 1171–1182, 2013.

[75] N. Bouhmaida, F. Bonhomme, B. Guillot, C. Jelsch, and N. E. Ghermani, "Charge density and electrostatic potential analyses in paracetamol," *Acta Crystallographica Section B Structural Science*, vol. 65, no. 3, pp. 363–374, 2009.

[76] I. M. Kenawi, "DFT analysis of diclofenac activity and cation type influence on the theoretical parameters of some diclofenac complexes," *Journal of Molecular Structure: THEOCHEM*, vol. 761, no. 1-3, pp. 151–157, 2006.

[77] R. N. Devi, A. D. Stephen, P. Justin, K. Saravanan, P. Macchi, and C. Jelsch, "Topological and electrostatic properties of diclofenac molecule as a non- steroidal anti-inflammatory drug: an experimental and theoretical study," *Journal of Molecular Structure*, vol. 1196, pp. 42–53, 2019.

[78] A. Jubert, M. L. Legarto, N. E. Massa, L. L. Tévez, and N. B. Okulik, "Vibrational and theoretical studies of non-steroidal anti-inflammatory drugs Ibuprofen [2-(4-isobutylphenyl)propionic acid]; naproxen [6-methoxy-α- methyl-2-naphthalene acetic acid] and tolmetin acids [1-methyl-5-(4-methylbenzoyl)-1H-pyrrole-2-acetic acid]," *Journal of Molecular Structure*, vol. 783, no. 1-3, pp. 34–51, 2006.

[79] A. E. Ahmed, L. M. Al-Harbi, G. O. Moustafa, M. A. El-Gazzar, R. F. Abdel-Rahman, and A. E. Salim, "Synthesis, comparative docking, and pharmacological activity of naproxen amino acid derivatives as possible anti-inflammatory and analgesic agents," *Drug Design, Development and Therapy*, vol. 13, pp. 1773–1790, 2019.